



# Corneal tissue properties following scleral lens wear using Scheimpflug imaging

Alejandra Consejo<sup>1</sup> , David Alonso-Caneiro<sup>2</sup>, Maciej Wojtkowski<sup>1</sup> and Stephen J Vincent<sup>2</sup> 

<sup>1</sup>Institute of Physical Chemistry, Polish Academy of Sciences, Warsaw, Poland, and <sup>2</sup>Contact Lens and Visual Optics Laboratory, School of Optometry and Vision Science, Queensland University of Technology, Brisbane, Australia

**Citation information:** Consejo A, Alonso-Caneiro D, Wojtkowski M, & Vincent SJ. Corneal tissue properties following scleral lens wear using Scheimpflug imaging. *Ophthalmic Physiol Opt* 2020; 40: 595–606. <https://doi.org/10.1111/opo.12710>

**Keywords:** corneal tissue, image statistical analysis, scheimpflug, scleral lenses

*Correspondence:* Alejandra Consejo  
E-mail address: alejandra.consejo@ichf.edu.pl

Received: 29 February 2020; Accepted: 26 May 2020; Published online: 23 July 2020

## Abstract

**Purpose:** To investigate the effect of short-term scleral lens wear on the corneal stroma at a macroscopic (thickness) and microscopic (within tissue) level, including regional variations.

**Methods:** Fourteen young, healthy participants wore a rotationally symmetric, 16.5 mm diameter, scleral lens for 8 h. Scheimpflug images were captured before, and immediately after, lens wear, and also on a second day (without lens wear) to quantify natural corneal diurnal variations. After corneal segmentation, pixel intensities of the stromal tissue were statistically modelled using a Weibull probability density function from which parameters  $\alpha$  and  $\beta$  were derived.

**Results:** Both  $\alpha$  and  $\beta$  parameters increased significantly following scleral lens wear (by  $5.7 \pm 10\%$  and  $6.5 \pm 6.5\%$ , respectively, both  $p < 0.01$ ). Corneal thickness also increased slightly following lens wear (mean increase  $0.49 \pm 1.77\%$ ,  $p = 0.01$ ); however, the change in  $\alpha$  and  $\beta$  parameters did not correlate with the magnitude of corneal swelling. On the control day, small but significant corneal thinning was observed ( $-0.82 \pm 1.1\%$ ,  $p = 0.03$ ), while  $\alpha$  and  $\beta$  parameters remained stable. Both microparameters varied significantly across the cornea, with  $\alpha$  decreasing ( $-15.4 \pm 0.7\%$ ) and  $\beta$  increasing towards the periphery ( $+4.4 \pm 2.6\%$ ) (both  $p < 0.001$ ).

**Conclusion:** Corneal microparameters  $\alpha$  and  $\beta$  varied regionally across the cornea and displayed a statistically significant increase following short-term scleral lens wear, but remained stable between morning and evening measurements taken during a control day without lens wear. These corneal microparameters may be a useful metric to quantify subclinical corneal changes associated with low level hypoxia.

## Introduction

Scleral lenses significantly improve visual acuity, vision-related quality of life, and corneal epithelial integrity across a wide range of ocular conditions.<sup>1</sup> In recent years, scleral lenses have increased in popularity amongst contact lens practitioners due to innovations in anterior segment imaging, improvements in rigid lens materials and manufacturing techniques, their various therapeutic use<sup>2</sup> and their increased availability worldwide.<sup>3</sup> However, since scleral lenses are substantially thicker than traditional corneal gas

permeable lenses,<sup>4</sup> and retain a sealed post-lens fluid reservoir with minimal tear exchange,<sup>5–7</sup> low level corneal oedema is still observed in modern daily scleral lens wear.<sup>8,9</sup> Scleral lenses also gradually settle back into the ocular surface during lens wear,<sup>10,11</sup> and due to their unique lens parameters and on eye fitting characteristics, behave differently to soft and rigid corneal lens designs.

Consequently, several studies have documented, in detail, the macroscopic anterior ocular tissue changes that occur following short-term scleral lens wear, including corneal swelling,<sup>8,9</sup> conjunctival and scleral tissue

compression,<sup>12,13</sup> and variations in corneal and corneal-scleral curvature.<sup>14–18</sup> However, to date, microscopic corneal changes (i.e. variations in intrinsic tissue properties) have not been reported. A more comprehensive characterisation of the corneal response to scleral lens wear should involve an *in-vivo* analysis of both the macroscopic and microscopic parameters. For example, recent studies have demonstrated that microstructural information from *in-vivo* corneal tissue can be extracted from both optical coherence tomography (OCT) (corneal speckle)<sup>19–22</sup> and Scheimpflug images (light intensity distribution).<sup>23,24</sup> This method is based on the statistical analysis of the pixel intensity distribution in corneal images and can differentiate between corneas of healthy individuals and those with keratoconus.<sup>23,24</sup>

The aim of this study is to investigate the effect of short-term scleral lens wear on corneal tissue at both a macroscopic and microscopic level. Corneal thickness is used to quantify macroscopic changes, while a previously validated method<sup>23,24</sup> is used to quantify microscopic changes within corneal tissue. In addition, local variations in these microscopic parameters across the cornea were investigated.

## Methodology

### Subjects and protocol

The protocol has been described in detail previously<sup>16</sup> and was approved by the Queensland University of Technology's University Human Research Ethics Committee and followed the tenets of the Declaration of Helsinki. All subjects gave written informed consent to participate. Briefly, 15 young, healthy participants (mean  $\pm$  SD: 22  $\pm$  3 years) with a range of refractive errors (left eye spherical equivalent from +0.50 to  $-4.50$  D) and at least 0.00 logMAR visual acuity in each eye were recruited (left eye visual acuity ranged from 0.00 to  $-0.20$  logMAR). Three of the participants wore soft contact lenses and ceased lens wear for at least 24 h prior to each measurement session. None of the participants wore rigid lenses. This study was conducted across three separate days. On the first day, participants were examined using a slit lamp biomicroscope to ensure suitability for scleral lens wear.

The optimal fitting diagnostic scleral lens (a rotationally symmetric Capricornia Irregular Corneal Design 16.5 mm total diameter, www.capcl.com.au) was then determined by following the manufacturer's fitting guide,<sup>25</sup> based on corneal sagittal height data extrapolated to a 15 mm chord<sup>26</sup> (the distance to the landing zone) and assessing the lens on the eye following a 1-h settling period. The lenses were manufactured in hexafocon A (Dk 100) and the thickness of the lens varied between some participants depending upon which sagittal depth was required (range of average lens thickness 334–407  $\mu$ m).<sup>4</sup> The second day served as a

control condition to quantify the natural corneal diurnal variation without lens wear. Scheimpflug images of the left eye were obtained using the Pentacam HR camera system (<https://www.oculus.de/en/frontpage/>) in the morning between 8:00 and 10:00 AM (at least 2 h after the participants reported time of waking) and again 8 h later between 4:00 and 6:00 PM. On the third day, Scheimpflug images of the left eye were obtained before the application of the optimal fitting scleral lens as determined on day one, and immediately after lens removal 8 h later. Reliable Scheimpflug imaging of corneal tissue cannot be obtained with a scleral lens on the eye due to the reflections from the surfaces of the contact lens. For this reason, Scheimpflug images were acquired immediately after lens removal. The timing of the day 2 and day 3 measurement sessions were matched for each participant. At each measurement session on days 2 and 3, five error free measurements were captured using the Pentacam HR using the 25-picture 3D scan mode. All participants completed the study, and wore the scleral lens continuously over an 8-h period with no complaints of midday fogging reported. However, one participant was excluded from this analysis since their day 3 final imaging session was conducted following the instillation of sodium fluorescein, which would affect the light intensity distribution of the Scheimpflug images.

### Data analysis

In addition to extracting the corneal thickness data provided by the built-in software, Scheimpflug images corresponding to 25 corneal meridians (a fixed size of 500  $\times$  1080 pixels) were exported for further analysis (i.e. 7000 images in total = 14 subjects  $\times$  2 measurement days  $\times$  2 sessions/day  $\times$  5 measurements/session  $\times$  25 meridians/measurement). The data analysis consists of two main stages: (1) corneal segmentation and (2) statistical modelling of the pixel light intensity distribution. Traditional image processing techniques, including a median filter and Canny edge detection, were used to remove the noise, extract the boundaries of interest and finally segment the corneal tissue (Figure 1). Thus, in this first stage, the segmentation method automatically extracts the anterior and posterior boundaries of the cornea.

Following the corneal segmentation, in the second stage a region of interest (ROI) was extracted automatically for statistical modelling. The ROI selection was delineated by the posterior corneal boundary and the anterior corneal boundary with an offset. This vertical (axial) offset ensured that the corneal epithelium was omitted from the ROI, since the epithelial tissue exhibits a different intensity distribution to that of the stroma,<sup>19</sup> which is the primary interest of this work since the corneal swelling response to modern scleral lens wear is almost entirely stromal.<sup>9</sup> Since

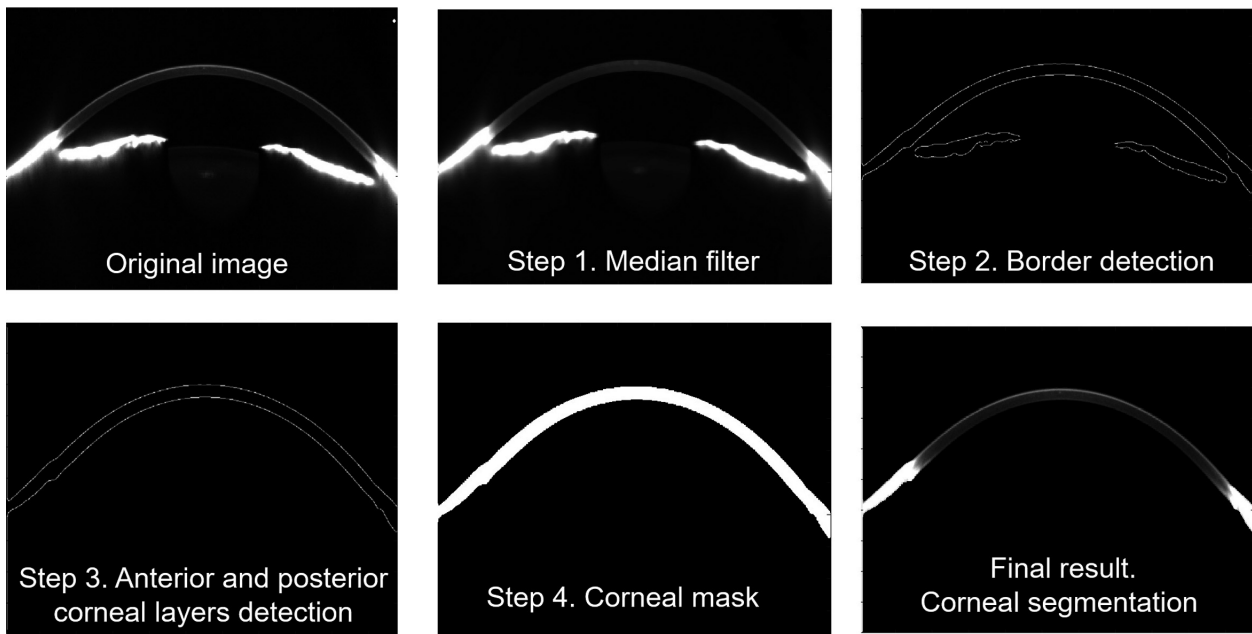


**Figure 1.** Main steps of the corneal segmentation of the Scheimpflug images.

the epithelial and anterior limiting lamina (Bowman’s) layers are difficult to distinguish in Scheimpflug images, it was decided to use an epithelial length offset equivalent to 12 % of the total central corneal thickness previously delineated by corneal segmentation.<sup>27</sup> Regarding the horizontal (lateral) dimension, a moving ROI of 11 pixels was applied across the cornea for each image as illustrated by *Figure 2a*. While a large moving ROI would limit the area under investigation (since not all pixels would be counted the same number of times), a small moving ROI would not provide sufficient data to fit the probability density function (PDF) adequately. As part of a preliminary analysis, the optimal length of the ROI was investigated. By moving the ROI one pixel, a significant change in  $\alpha$  from one ROI

to the adjacent one should not occur. Therefore, a change in  $\alpha$  between two consecutive ROIs larger than 0.25 (approximately 0.5% variation of  $\alpha$ ) was considered potential noise. The number of pixels in the ROI was iteratively increased by one until this condition was met. The first pixel length to meet this condition (11 pixels) was consequently chosen for further analysis. The moving ROI covered approximately the central 8 mm of the cornea. To avoid undesired border effects (strong limbal/ scleral reflections) the peripheral cornea was not included in the ROI. Besides calculating the mean pixel intensity (MPI) distribution, pixels corresponding to a given ROI were modelled using a distribution function and, for illustrative purposes only, grouped in a histogram according to pixel intensity,

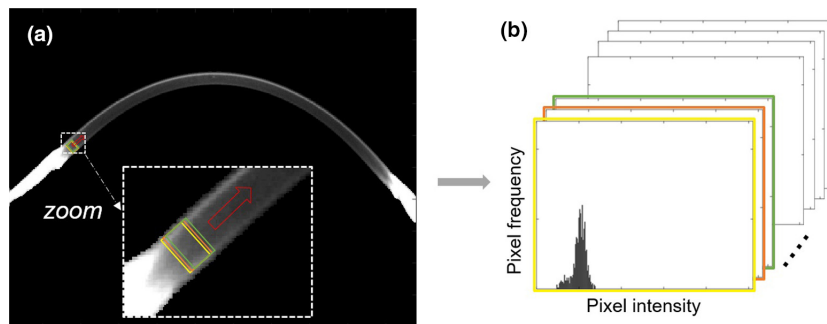


**Figure 2.** Moving region of interest (ROI) analysis process (a) and corresponding collection of histograms representing pixel intensity distribution in each ROI (b). For illustrative purposes, only the first three ROIs are shown with different colours along with a red arrow that indicates the continuity of the process across the segmented cornea (a). The histogram corresponding to the first selected ROI is shown in the foreground (b).  $\alpha$  and  $\beta$  parameters were obtained from each distribution function (from each ROI) and later averaged.

Figure 2b. Pixel intensity indicates how bright a given pixel is, and depends on the scattering light intensity. Pixel intensity distribution of each ROI was approximated by the two-parameter distribution functions that were previously used in the statistical analysis of corneal images (i.e., Weibull, Gamma and Lognormal distribution).<sup>19</sup> To assess which was the optimal function from the three candidates, the goodness of the fit (GoF) was determined by the root mean square error (RMSE), with a lower RMSE indicating a better GoF. The RMSE was slightly lower using a Weibull function ( $0.005 \pm 0.001$ ) than Gamma ( $0.007 \pm 0.001$ ) or Lognormal ( $0.007 \pm 0.001$ ) distributions. Consequently, the Weibull PDF was used and is defined as,

$$f(x) = \frac{\beta}{\alpha} \left(\frac{x}{\alpha}\right)^{\beta-1} e^{-\left(\frac{x}{\alpha}\right)^\beta} \text{ if } x \geq 0 \text{ or } 0 \text{ otherwise} \quad (1)$$

where the independent variable ( $x$ ) represents pixel intensity,  $\alpha > 0$  represents the scale parameter and  $\beta > 0$  represents the shape parameter. Both parameters were estimated using the method of maximum likelihood from the pixel intensities of every ROI in each image. Thus, the  $\alpha$  and  $\beta$  parameters were obtained from each distribution function (from each ROI as indicated by Figure 2b) and later averaged. In summary, parameters  $\alpha$  and  $\beta$  are derived from the statistical analysis of light intensity distribution of corneal Scheimpflug images. Generally speaking, a change in the scale parameter ( $\alpha$ ) causes a displacement of the pixel intensity distribution along the pixel intensity axis ( $x$ -axis). In other words, an increase and decrease in  $\alpha$  corresponds to an increase and decrease in pixel intensity, respectively. On the other hand, a change in the shape parameter ( $\beta$ ) affects the width of the pixel intensity distribution. The smaller the  $\beta$ , the greater the spread of the pixel intensity distribution of a given image, while a large  $\beta$  indicates greater similarity in pixel intensities within a given image.

The Weibull model provides parameters  $\alpha$  and  $\beta$  that have a physical interpretation.<sup>19</sup> In particular, it has been suggested that the scale parameter may account for the scatter density while the shape parameter may account for the cross-section of the scattered element.<sup>19</sup> In other words, if one considers the cornea as comprised of small scattering elements,  $\beta$  would indicate their number and  $\alpha$  their size.

Further, to investigate regional corneal changes, after transformation to polar coordinates, data were interpolated, smoothed using second-order Zernike polynomials, and the corresponding regional maps of  $\alpha$  and  $\beta$  parameters were obtained. The central cornea (4 mm diameter), peripheral cornea (4–8 mm annulus) and the entire central cornea (8 mm) were considered. These corneal regions were further divided into four sectors for statistical analysis: superior (S) [45, 135]°, inferior (I) [225, 315]°, nasal (N) [315, 45]° and temporal (T) [135, 225]°. Corneal thickness

regional maps were not considered in this work, as these have been reported elsewhere.<sup>7</sup>

### Statistical analysis

The statistical analysis was performed using SPSS statistics software (<https://www.ibm.com/analytics/spss-statistics-software>). The Shapiro–Wilk test indicated that all variables were not normally distributed. Consequently, the Wilcoxon signed-rank test was performed to determine the statistical significance of differences in the parameters under investigation between the morning (before wear) and evening session (after lens wear). The same test was applied to investigate baseline differences between the control (day 2, morning session) and the lens wearing day (day 3, prior to lens wear). The Wilcoxon signed-rank test was also used to investigate regional corneal changes of  $\alpha$  and  $\beta$  parameters. Bonferroni corrections were used to overcome inflation due to multiple comparisons by dividing the significance level by the number of comparisons performed ( $N = 121$ ). Consequently, when Bonferroni correction was used the alpha error per comparison was 0.0004 (0.05/121). For clarity, Bonferroni corrections are indicated in the text. In addition, regression analysis was used to investigate the correlation of microscopic parameters (baseline values of  $\alpha$  and  $\beta$  and the change of those parameters within sessions) with macroscopic parameters (baseline corneal thickness and corneal swelling). The coefficient of variation (CoV) was calculated for each parameter analysed (corneal thickness, MPI,  $\alpha$  and  $\beta$  parameters) using the five repeated values obtained at each session. The level of significance was set to 0.05.

## Results

### Intrasession repeatability

Using the five repeated measurements, all analysed parameters displayed good intrasession repeatability with coefficients of variation of 0.7 % for corneal thickness, 1.8 % for  $\alpha$ , 4.1 % for  $\beta$  and 2.5 % for MPI.

### Variations in corneal macroscopic and microscopic parameters

No statistically significant differences were observed between the baseline (morning) corneal parameters measured on days 2 and 3:  $\alpha$  (Wilcoxon signed-rank test,  $p = 0.53$ ),  $\beta$  ( $p = 0.51$ ), MPI ( $p = 0.60$ ), and corneal thickness ( $p = 0.82$ ).

### Diurnal variations

During the control day, without scleral lens wear (averaged across the central 8 mm) no statistically significant changes

were observed in the  $\alpha$  and  $\beta$  parameters or MPI (Table 1), while the cornea thinned over the course of the day ( $-9 \pm 9 \mu\text{m}$ ,  $p = 0.026$ ) (Table 1).

### Effect of scleral lens wear

Scleral lens wear had a statistically significant effect on both macroscopic and microscopic corneal parameters (Table 1). Individual changes in  $\alpha$  and  $\beta$  parameters are shown in Table 2. Averaged over the central 8 mm, corneal thickness increased by  $+3 \pm 9 \mu\text{m}$  ( $p = 0.010$ ),  $\alpha$  increased by  $+3.12 \pm 2.7$  a.u. ( $p < 0.001$ ),  $\beta$  increased by  $+0.37 \pm 0.53$  a.u. ( $p = 0.009$ ), and MPI increased by  $+2.11 \pm 2.7$  a.u. ( $p < 0.001$ ). Taking into consideration the natural diurnal variations measured on day 2, the total effect of scleral lens wear on these corneal parameters was a  $12 \pm 4.12 \mu\text{m}$  increase in corneal thickness, a  $3.85 \pm 4.48$  arbitrary units (a.u.) increase in  $\alpha$ , a  $+0.17 \pm 2.96$  a.u. increase in  $\beta$ , and a  $+2.67 \pm 6.50$  a.u. increase in MPI.

The corneal microscopic parameters investigated ( $\alpha$  and  $\beta$ ) were not correlated with corneal thickness. This phenomenon was observed repeatedly across the various measurement sessions. Specifically, for the baseline session on control day ( $\alpha$ :  $R^2 = 0.01$ ,  $p = 0.37$ ;  $\beta$ :  $R^2 = 0.01$ ,  $p = 0.37$ ), the evening session on control day ( $\alpha$ :  $R^2 = 0.01$ ,  $p = 0.37$ ;  $\beta$ :  $R^2 = 0.02$ ,  $p = 0.31$ ), the baseline session on lens-wearing-day ( $\alpha$ :  $R^2 = 0.10$ ,  $p = 0.14$ ;  $\beta$ :  $R^2 = 0.02$ ,  $p = 0.31$ ) and the corresponding evening session after lens removal ( $\alpha$ :  $R^2 = 0.01$ ,  $p = 0.37$ ;  $\beta$ :  $R^2 = 0.03$ ,  $p = 0.28$ ). Likewise, no correlation was found between lens-wearing day baseline values of  $\alpha$  or  $\beta$  with

**Table 2.** Individual change in  $\alpha$  and  $\beta$  parameters as a consequence of scleral lens wear for each of the 14 participants

No.	Before lens wear		After lens wear		Difference (a.u.)	
	$\alpha$	$\beta$	$\alpha$	$\beta$	$\alpha$	$\beta$
01	52.04	5.74	53.01	6.16	0.97	0.43
02	48.64	6.09	67.70	7.34	19.07	1.25
03	50.01	4.13	53.03	4.08	3.02	-0.06
04	52.75	5.63	52.53	5.68	-0.22	0.06
05	51.91	5.32	54.68	5.40	2.78	0.08
06	55.18	5.34	56.37	5.20	1.36	-0.14
07	60.93	5.32	63.18	5.73	2.60	0.41
08	57.19	4.57	60.23	5.15	3.04	0.57
09	54.60	5.17	55.17	5.81	4.54	0.64
10	57.72	5.71	63.26	5.86	0.57	0.15
11	53.44	4.83	62.02	5.18	8.58	0.35
12	55.45	5.87	59.65	5.94	4.20	0.07
13	57.53	5.07	54.40	4.95	-3.13	-0.12
14	64.01	6.20	64.56	6.82	0.55	0.62
Overall	54.89	5.33	58.01	5.70	3.12	0.37
	[52.01, 57.58]	[5.01, 5.77]	[54.06, 63.20]	[5.17, 5.99]	[0.57, 4.53]	[0.03, 0.58]

Values acquired from five consecutive images per session were used to describe the individual values. 'Overall' row represents the median value of the individual values (1–14) presented in the table with their correspondent interquartile range (IQR).

$\alpha$  and  $\beta$  – arbitrary units (a.u.).

corneal swelling ( $\alpha$ :  $R^2 = 0.06$ ,  $p = 0.20$ ;  $\beta$ :  $R^2 = 0.01$ ,  $p = 0.37$ ). Similarly, no correlation was found between the change observed in  $\alpha$  and/or  $\beta$  parameters (difference

**Table 1.** Median values of  $\alpha$  and  $\beta$  parameters, mean pixel intensity (MPI) and corneal thickness (CT). During the control day and before and after wearing scleral lenses (SL) for 8 mm central cornea of 14 participants

	Morning median [IQR]	Evening median [IQR]	Difference median	Percentage change median	<i>p</i> -value (Wilcoxon signed-rank test)
Control day					
$\alpha$	53.41 [50.62, 57.49]	52.68 [50.33, 57.62]	-0.73	-1.37	0.44
$\beta$	5.39 [4.93, 5.78]	5.59 [5.19, 5.84]	0.20	3.71	0.085
MPI	49.16 [46.70, 53.08]	48.60 [46.48, 52.82]	-0.56	-1.13	0.49
CT ( $\mu\text{m}$ )	614 [575, 639]	607 [570, 633]	-5	-0.82	0.026
Scleral lens wear day					
$\alpha$	54.89 [52.01, 57.58]	58.01 [54.06, 63.33]	3.12	5.68	<0.001
$\beta$	5.33 [5.01, 5.77]	5.70 [5.17, 5.99]	0.37	6.49	0.009
MPI	50.55 [48.20, 53.95]	52.66 [49.56, 58.48]	2.11	4.17	<0.001
CT ( $\mu\text{m}$ )	617 [576, 640]	620 [585, 643]	3	0.49	0.010

$\alpha$ ,  $\beta$  and MPI – arbitrary units. Percentage change is evening minus morning measurement and the denominator is baseline (morning) value.

$\alpha$ ,  $\beta$  and MPI – arbitrary units. Percentage change is post lens wear minus pre lens wear measurement and the denominator is baseline (pre lens) value.

IQR, interquartile range.



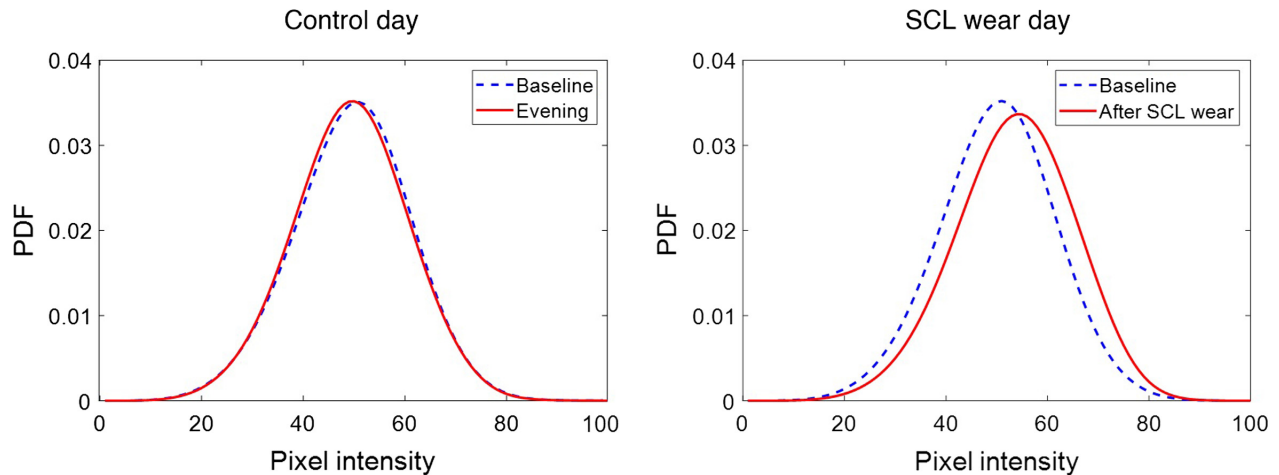


**Figure 3.** Mean probability density function (PDF) of the Weibull distribution of the horizontal meridian for the 14 participants. Left: control day (blue morning baseline measurement, red evening measurement); Right: lens wear day (blue before lens insertion, red after lens removal).

between evening/baseline sessions on lens wearing day) with thickness change ( $\alpha$ :  $R^2 = 0.14$ ,  $p = 0.09$ ;  $\beta$ :  $R^2 = 0.02$ ,  $p = 0.31$ ).

Figure 3 (right side) illustrates the mean Weibull PDF comparing before (dashed blue line) and after scleral lens wear (solid red line). Short-term lens wear expanded the distribution around its centre and caused a shift towards a higher pixel intensity ( $p = 0.001$ ). No significant diurnal variations were observed in the mean PDF on the control day without lens wear (Figure 3, left side,  $p = 0.85$ ).

Although the statistical analyses revealed significant changes in both  $\alpha$  and  $\beta$  corneal parameters following lens wear (Table 1, Figure 3), some variability in the magnitude of change was observed between participants as shown in Table 2. Figure 4 displays the probability distribution functions for two different participants to highlight this effect; one from whom noticeable changes in  $\alpha$  and  $\beta$  parameters following lens wear were not found (Figure 4, top left plot-S01) and another from whom noticeable changes were found (Figure 4, top right plot-S02). The corresponding results during the control day (no lens on the eye) are also displayed.

### Regional analysis

Figure 5 displays the group median change in  $\alpha$  and  $\beta$  parameters in the baseline measurement and immediately after lens removal across the central 8 mm of the cornea. Table 3 shows the corresponding statistical analysis. Parameters  $\alpha$  and  $\beta$  show local variations across the cornea. Analysis of the morning (baseline) maps revealed that  $\alpha$  was  $15.4 \pm 0.7$  % higher in central cornea compared to the periphery. Conversely,  $\beta$  was  $4.4 \pm 2.6$  % lower in central cornea compared to the periphery. Regarding the different corneal sectors, statistically significant differences were

found when comparing I-N, I-S, I-T, N-S, N-T, S-T (Wilcoxon signed-rank test; all  $p < 0.004$  [Bonferroni]) for both  $\alpha$  and  $\beta$  baseline maps, independent of the region analysed (central 0-4 mm, peripheral 4-8 mm annulus, or the entire central 8 mm of the cornea).

The effect of lens wear upon corneal microparameters was greatest in the peripheral cornea for both  $\alpha$  ( $5.7 \pm 0.9$  %) and  $\beta$  ( $6.3 \pm 1.7$  %), in comparison to the central cornea,  $\alpha$  ( $3.6 \pm 0.8$  %) and  $\beta$  ( $5.2 \pm 0.4$  %). Regarding the different corneal sectors, the greatest changes in microparameters were observed nasally, and the least amount of change occurred temporally (Table 3).

### Discussion

This is the first study to investigate *in-vivo* corneal tissue changes as a consequence of short-term scleral lens wear at both a macroscopic and microscopic level. A pair of novel parameters ( $\alpha$  and  $\beta$ ), recently introduced to better understand Scheimpflug light intensity distribution in eyes with keratoconus,<sup>23,24</sup> were used to quantify corneal changes within the stroma at the microscopic level. Both parameters increased significantly following lens wear (Table 1, Figure 3, Figure 5), in addition to corneal swelling. Previous research has demonstrated that short-term hypoxia alters proteoglycan metabolism, which can affect the arrangement of collagen fibres within the stroma.<sup>28</sup> The results of the current work show that the light scattering properties of the stroma were altered as a consequence of lens wear. This study does not provide sufficient data to assess the origin of the observed differences in pixel intensity distributions as a consequence of lens wear. However, based on previous studies that have shown that lens induced hypoxia alters collagen fibril arrangement,<sup>29,30</sup> it is highly likely that

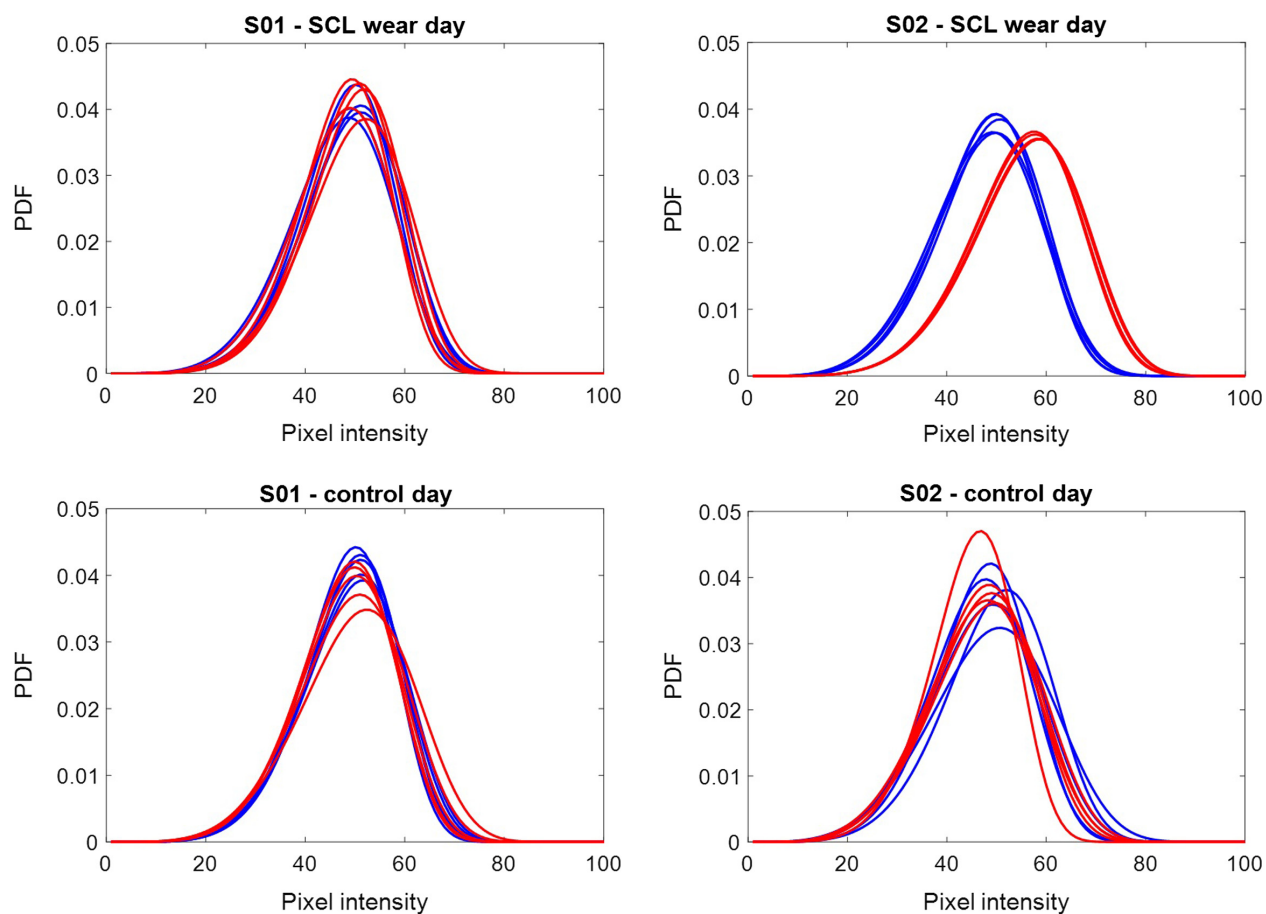


**Figure 4.** Comparison in probability density distribution (PDF) of the Weibull distribution of the horizontal meridian of a participant (S01, left) from whom noticeable changes in  $\alpha$  and  $\beta$  parameters following lens wear were not found as a consequence of scleral lens wear (SL) and a participant (S02, right) from whom noticeable changes were found. Bottom: control day; Top: scleral lens (SL) wear day. The five PDFs represent data from each Pentacam HR measurement at each time point. Blue denotes baseline/before scleral lens wear, red denotes evening/after scleral lens wear.

light scattering properties of the stroma were altered as a consequence of lens induced hypoxia. In particular, the observed increment in  $\alpha$  translates to more corneal backscattering (i.e., a less transparent stroma) while the observed increment in  $\beta$  indicates that this change affects the whole stroma. Individual differences were observed among participants (Table 2 and Figure 4). The stroma of all participants was not equally affected as a consequence of short-term scleral lens wear. That is, not all of the participants had the same hypoxic response to the lens wear. However, the fundamental cause of this inter-subject variation goes beyond the scope of the current work. The maps plotted in Figure 5 represent the median group value, meaning that the group parameters for one condition were always greater at every point across the cornea. However, if individual differences were plotted this would not always be the case.

Similar to the current study, Jesus and Iskander<sup>19</sup> applied a statistical modelling approach to examine corneal micro-

structural changes *in-vivo* using a speckle field generated by corneal microstructure in OCT images. In a small sample of subjects ( $n = 4$ , mean age 38 years), OCT images were obtained before and after 3 h of low Dk soft contact lens wear and patching over the closed eye. More than 8 % corneal swelling was induced on average, which resulted in significant variations in various shape parameters (~17-30% change). In the same work, the authors also observed that corneal macroscopic (thickness) and microscopic parameters were not directly correlated and did not recover at the same rate following the removal of the hypoxic stimulus.<sup>19</sup> The fact that microscopic and macroscopic corneal parameters were not correlated is consistent with the current study, in which scleral lens induced changes in  $\alpha$  and  $\beta$  parameters were not significantly associated with corneal swelling ( $\alpha$ :  $R^2 = 0.06$ ,  $p = 0.20$ ;  $\beta$ :  $R^2 = 0.01$ ,  $p = 0.37$ ). The independence of corneal thickness from  $\alpha$  and  $\beta$  parameters has also been demonstrated in previous work investigating  $\alpha$  and  $\beta$  parameters in keratoconic and healthy

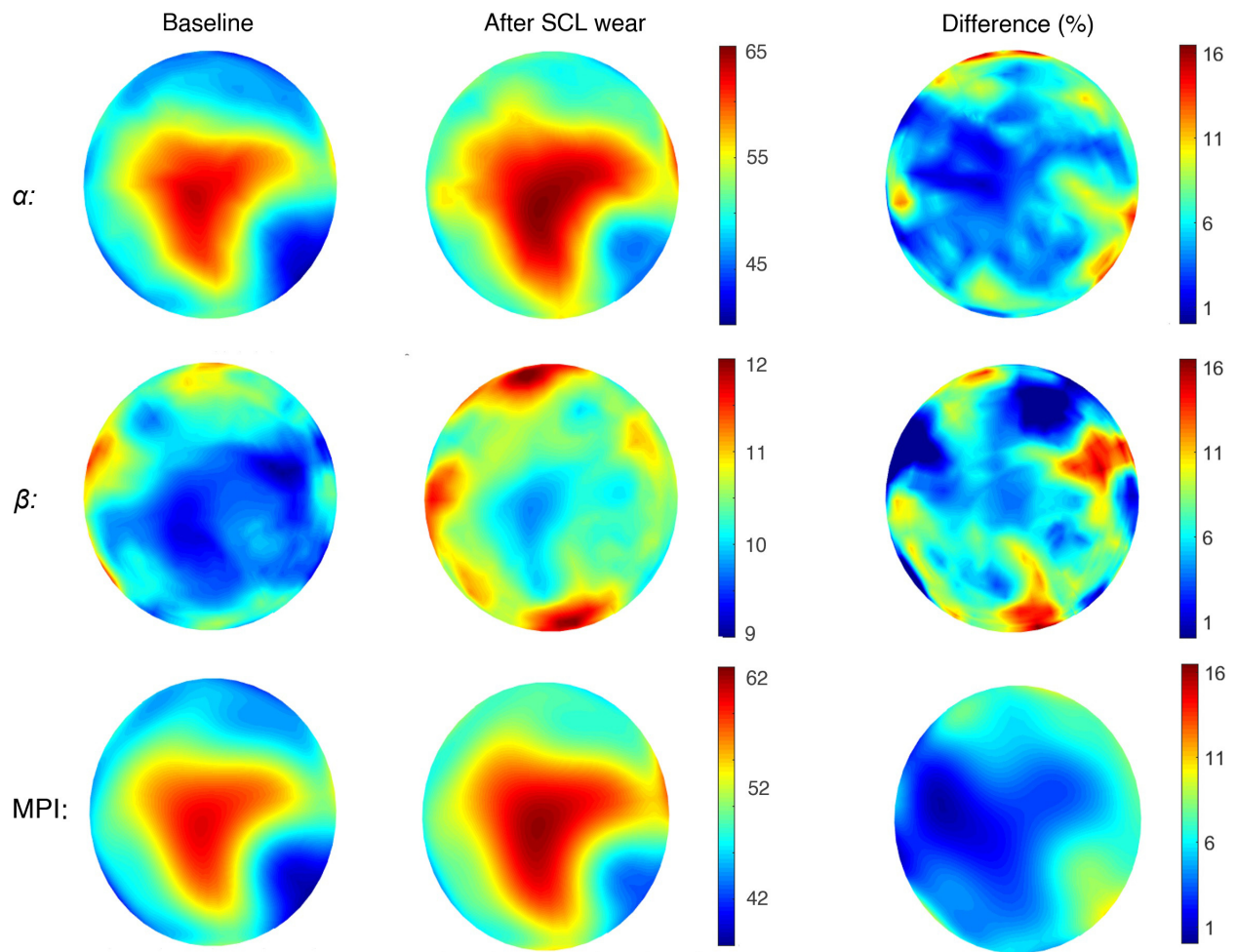


**Figure 5.** The median distribution of  $\alpha$  and  $\beta$  parameters and mean pixel intensity (MPI) in the 8 mm central cornea of the 14 participants. Left: pre-scleral lens wear; Middle: immediately after 8 h of scleral lens wear; Right: median percentage difference (post-lens wear minus pre-lens wear. Pre-lens wear is the denominator). Colour bars for pre- and post-lens wear are expressed in arbitrary units. Colour bars for the difference maps are percentage change.

eyes using Scheimpflug imaging.<sup>24</sup> In that work, a bootstrap analysis was performed which indicated that not only are macroscopic and microscopic parameters independent from each other, but also that corneal thickness is not a confounding factor that affects the calculation of  $\alpha$  and  $\beta$ .<sup>24</sup> Ultimately, to prove that the observed changes in  $\alpha$  and  $\beta$  are related to hypoxia, rather than fluid mechanics, requires an additional experiment using a range of soft contact lenses (from low to high Dk) to induce varying degrees of corneal hypoxia, without the thick post-lens fluid reservoir that occurs with scleral lenses. Although a soft lens control group was not included in this study, Jesus and Iskander<sup>19</sup> applied a similar modelling approach (a Gamma distribution) to OCT speckle data obtained before and after soft contact lens wear and observed similar highly significant changes in their model parameters. This supports the

hypothesis that the observed changes in the current study are most likely a result of corneal hypoxia rather than post-lens reservoir fluid mechanics.

The parameters  $\alpha$  and  $\beta$  remained stable comparing the morning and evening session in the control day without lens wear ( $-1.37$  to  $+3.71$  % variation), despite a small but statistically significant amount of corneal thinning of  $\sim 0.8$  % (Table 1, Figure 3). Jesus and Iskander<sup>19</sup> also observed minimal change in similar shape parameters associated with OCT derived corneal speckle in a control condition;  $0.6$  % corneal thinning and  $-4.3$  to  $+3.1$  % variation in their shape parameters. This suggests that a certain magnitude of hypoxic stress or corneal oedema must be reached before significant optical changes in the stroma become detectable (i.e. greater than  $\sim 0.8$  % tissue swelling).



**Table 3.** Median  $\pm$  SD regional differences in central cornea (4 mm diameter) and peripheral cornea (annulus 4–8 mm) in  $\alpha$  (top) and  $\beta$  (bottom) parameters for the left eye of 14 participants who wore a scleral lens during an 8-h period

	Before lens wear			After lens wear			p-value (Baseline vs evening)	
	Central cornea	Peripheral cornea	p-value (central vs peripheral)	Central cornea	Peripheral cornea	p-value (central vs peripheral)	Central cornea	Peripheral cornea
$\alpha$								
Inferior	59 $\pm$ 3	49 $\pm$ 3	<0.0004	61 $\pm$ 3	52 $\pm$ 2	<0.0004	<0.0004	<0.0004
Nasal	59 $\pm$ 3	50 $\pm$ 4	<0.0004	62 $\pm$ 2	53 $\pm$ 4	<0.0004	<0.0004	<0.0004
Superior	60 $\pm$ 3	51 $\pm$ 5	<0.0004	63 $\pm$ 3	54 $\pm$ 5	<0.0004	<0.0004	<0.0004
Temporal	61 $\pm$ 2	52 $\pm$ 3	<0.0004	63 $\pm$ 2	54 $\pm$ 3	<0.0004	<0.0004	<0.0004
$\beta$								
	Central cornea	Peripheral cornea	p-value (central vs peripheral)	Central cornea	Peripheral cornea	p-value (central vs peripheral)	Central cornea	Peripheral cornea
Inferior	9.7 $\pm$ 0.3	10.3 $\pm$ 0.3	<0.0004	10.2 $\pm$ 0.2	10.7 $\pm$ 0.4	<0.0004	<0.0004	<0.0004
Nasal	9.6 $\pm$ 0.1	9.7 $\pm$ 0.3	<0.0004	10.1 $\pm$ 0.1	10.5 $\pm$ 0.2	<0.0004	<0.0004	<0.0004
Superior	9.6 $\pm$ 0.2	9.9 $\pm$ 0.3	<0.0004	10.1 $\pm$ 0.2	10.6 $\pm$ 0.4	<0.0004	<0.0004	<0.0004
Temporal	9.5 $\pm$ 0.2	10.2 $\pm$ 0.4	<0.0004	9.9 $\pm$ 0.2	10.7 $\pm$ 0.3	<0.0004	<0.0004	<0.0004

Wilcoxon signed-rank test was applied to determine statistical significant differences. Bonferroni correction was also considered ( $\alpha_{\text{per comparison}} = 0.0004$ ).

This is the first study to investigate the regional distribution of  $\alpha$  and  $\beta$  parameters across the central 8 mm of the cornea (Figure 5). Both  $\alpha$  and  $\beta$  parameters varied towards the periphery, across all quadrants (Table 3). The greatest changes in both  $\alpha$  and  $\beta$  parameters following lens wear were found nasally ( $\alpha$ : ~5.8 %;  $\beta$ : ~6.7 %) and the smallest changes were observed temporally ( $\alpha$ : ~3.5 %;  $\beta$ : ~4.7 %). It is known that fibrils in the peripheral cornea are more abundant<sup>31,32</sup> and larger in diameter than those from the central cornea.<sup>32</sup> In addition, previous research has demonstrated that the reduced transparency in the peripheral stroma is primarily caused by changes in fibril radius.<sup>33,34</sup> These studies showed that the increase in fibril radius has a greater effect on light propagation through the stroma, and such influence is likely to be the source of the decrease in light transmission as a function of position seen in the peripheral regions.<sup>33</sup> This difference in tissue composition would alter how the light travels through the tissue,<sup>33</sup> and consequently modify  $\alpha$  and  $\beta$  parameters. Similar to traditional densitometry, pixel intensity distribution that is modelled using a Weibull function, is based on the backscattering of light. Generally speaking, light from the source reaches the object to be imaged (the cornea), which is partially backscattered towards the detector to form an image. This final image therefore depends on how light travels within the cornea and how much of it is backscattered. The arrangement of corneal components (such as epithelial cells, keratocytes, proteoglycans, collagen fibrils,

and endothelial cells) would cause light to travel differently within the different layers and regions, resulting in intensity differences in the final image. Those pixel intensity differences can be statistically modelled to infer tissue characteristics. Although many statistical models could be suitable for this purpose,<sup>19</sup> the Weibull function was chosen since it showed a good fit for Scheimpflug images, in accordance with previous research.<sup>24</sup>

Since  $\alpha$  and  $\beta$  parameters provide information on tissue transparency, the newly introduced corneal regional maps of  $\alpha$  and  $\beta$  parameters could be of use to further investigate ocular diseases where localised changes in corneal structure occurs, such as keratoconus. As an alternative to regional analysis, Figure 3 shows microstructural changes in a single meridian. The mean PDF of the Weibull distribution of the horizontal meridian for the 14 participants is plotted in Figure 3 to illustrate that valuable information can be extracted from one image along a single meridian per participant.

Mean pixel intensity and  $\alpha$  were found to be statistically significant different from each other, independent of the session (lens day: morning and evening (both  $p < 0.001$ ), scleral lens wear day: before and after lens wear (both  $p < 0.001$ )). However, both MPI and  $\alpha$  displayed a very similar regional distribution pattern as illustrated in Figure 5. Since, by definition, the mean value of a Weibull PDF is proportional to the scale parameter ( $\alpha$ ),<sup>35</sup> this result was expected. One could question the added value of the

proposed methodology (modelling the pixel intensity distribution with a Weibull function), versus simply calculating the mean value of that pixel intensity distribution. In this regard, it is important to notice that first, in the current study  $\alpha$  was found to be more sensitive than MPI to changes produced as a consequence of scleral lens wear (Figure 5, right). Secondly, the pixel intensity distribution was not normally distributed. From a statistical point of view, calculating the mean of a non-normal distribution might lead to bias, thus care should be exercised while analysing the MPI data. Although other statistical parameters (such as median, skewness, kurtosis) could be considered, a parametric model, such as Weibull, is generally more robust towards outliers.<sup>36</sup> In this work  $\alpha$  showed a better (lower) coefficient of variation than MPI.

A limitation of the current study is that all participants were young and healthy with normal corneas, and no history of ocular disease or scleral lens wear. Consequently, the results must be interpreted with caution and may not be applicable for older patients, those with ocular surface abnormalities, corneal disease or regular contact lens wearers. In addition, no further serial measurements were performed after the initial lens removal, and consequently the recovery rate of the observed changes should be considered in future studies. Also, scleral lens removal could potentially induce some ocular surface inflammation in neophyte lens wearers; however, such stress would most likely occur towards the sclera where pressure is applied to remove the lens. In the current study, an experienced optometrist conducted lens removal without complications. The relationship between changes in corneal microscopic parameters and visual function, as well as the influence of the type of contact lens worn, should also be investigated. Given the low level of oedema observed in the current study, more sensitive measures than high contrast visual acuity would likely be required to quantify the visual effect of such changes (e.g. contrast sensitivity or subjective measures of light scatter).<sup>37,38</sup> However, it is important to bear in mind that the work from Mitchell & Elliott<sup>38</sup> is based on the van den Berg straylight meter, which differs from the backscatter of slit-lamp and Scheimpflug in that it measures forward light scatter. Forward light scattering refers to light scattered from the cornea and lens towards the retina. It may be much greater than backscattered light, unless is Rayleigh scatter<sup>39</sup> and depends on the microstructure of the medium.<sup>39</sup> The relationship of forward light scattering to backward light scattering is the light scattering seen during slit lamp examination or Scheimpflug images. In the current work, we chose to exclusively analyse the stromal area, since it has been reported that that the epithelial and endothelial tissue exhibit increased backscatter to that of the

stroma,<sup>40</sup> which is the primary interest of this work since the corneal swelling response to modern scleral lens wear is almost entirely stromal.<sup>9</sup> However, there is no technical constraint to also analyse other corneal layers.

A potential technical limitation of this work is the analysis using the moving ROI shifts by one pixel, as illustrated in Figure 2a. Consequently, most individual pixels are counted multiple times, except for those pixels in the peripheral cornea, which are counted fewer times. Since the moving ROI is 11 pixels in length, this would affect the 10-most-peripheral pixels in each corneal image (i.e. approximately 0.2 mm from the 8 mm analysed, or 2.5%). The length of the ROI (11 pixels) was chosen after considering this limitation. On the other hand, the results reported should be put in context of the inherent noise of the imaging device. Overall, all analysed parameters displayed good intrasession repeatability across the five repeated measures. The  $\beta$  parameter showed a higher coefficient of variation (4.1%) than the  $\alpha$  parameter (1.8%), which likely explains the variation in PDF height in some of the subplots of Figure 4 which showed higher variability on day 2 (control day) than day 3 (scleral lens wear day) for the same participant. Assessing the inherent noise of the imaging system of the Pentacam device is beyond the scope of the current work, but it would be of interest to investigate this in the future.

Hypoxia as a consequence of scleral lens wear is a common clinical problem for practitioners that has been repeatedly investigated using different experimental approaches.<sup>7,8,15</sup> Clinical trials including neophyte and regular lens wearers, healthy and compromised eyes, and also different mathematical models have been used to try to understand oxygen delivery during lens wear and the physiological changes that occur in the cornea. The methods used in the current study utilise an alternative approach to previous investigations, which provide new insights into microstructural corneal changes that are likely linked to optical quality. On average, the change in corneal thickness observed following lens wear (1.3% oedema relative to the control day) would not be considered clinically significant for young healthy eyes in the short-term, and would be undetectable during routine slit lamp examination. The method described in this paper allows the quantification of microstructural corneal changes that occur following short-term scleral lens wear, with minimal oedema.

In conclusion, despite minimal corneal oedema, following 8 h of scleral lens wear, statistically significant changes were observed within corneal stromal tissue properties. Although the clinical implication of these changes requires further experimentation, these microparameters may be a useful additional metric to monitor subclinical corneal changes in response to low grade hypoxia.

## Acknowledgements

This project has received funding from the European Union's Horizon 2020 research and innovation program under grant agreement No 779960.

## Conflict of interest

The authors report no conflicts of interest and have no proprietary interest in any of the materials mentioned in this article.

## References

- Pullum KW, Whiting MA & Buckley RJ. Scleral contact lenses: the expanding role. *Cornea* 2005; 24(3): 269–277.
- Sabesan R, Johns L, Tomashevskaya O, Jacobs DS, Rosenthal P & Yoon G. Wavefront-guided scleral lens prosthetic device for keratoconus. *Optom Vis Sci* 2013; 90(4): 314–323.
- Vincent SJ. The rigid lens renaissance: a surge in sclerals. *Cont Lens Anterior Eye* 2018; 41(2): 139–143.
- Vincent SJ, Alonso-Caneiro D, Kricancic H & Collins MJ. Scleral contact lens thickness profiles: The relationship between average and centre lens thickness. *Cont Lens Anterior Eye* 2019; 42(1): 55–62.
- Paugh JR, Chen E, Heinrich C *et al.* Silicone hydrogel and rigid gas-permeable scleral lens tear exchange. *Eye Contact Lens* 2018; 44(2): 97–101.
- Vincent SJ, Alonso-Caneiro D & Collins MJ. Regional variations in postlens tear layer thickness during scleral lens wear. *Eye Contact Lens* 2019. <https://doi.org/10.1097/ICL.0000000000000676> [Epub ahead of print].
- Tan B, Zhou Y, Yuen TL, Lin K, Michaud L & Lin MC. Effects of scleral-lens tear clearance on corneal edema and post-lens tear dynamics. *Optom Vis Sci* 2018; 95(6): 481–490.
- Vincent SJ, Alonso-Caneiro D, Collins MJ *et al.* Hypoxic corneal changes following eight hours of scleral contact lens wear. *Optom Vis Sci* 2016; 93: 293–299.
- Vincent SJ, Alonso-Caneiro D & Collins MJ. The time course and nature of corneal oedema during sealed miniscleral contact lens wear. *Cont Lens Anterior Eye* 2019; 42(1): 49–54.
- Vincent SJ, Alonso-Caneiro D & Collins MJ. The temporal dynamics of miniscleral contact lenses: central corneal clearance and centration. *Cont Lens Anterior Eye* 2018; 41(2): 162–168.
- Bray C, Britton S, Yeung D, Haines L & Sorbara L. Change in over-refraction after scleral lens settling on average corneas. *Ophthalmic Physiol Opt* 2017; 37(4): 467–472.
- Alonso-Caneiro D, Vincent SJ & Collins MJ. Morphological changes in the conjunctiva, episclera and sclera following short-term miniscleral contact lens wear in rigid lens neophytes. *Cont Lens Anterior Eye* 2016; 39(1): 53–61.
- Consejo A, Behaegel J, Van Hoey M, Iskander DR & Rozema JJ. Scleral asymmetry as a potential predictor for scleral lens compression. *Ophthalmic Physiol Opt* 2018; 38(6): 609–616.
- Consejo A, Behaegel J, Van Hoey M, Wolffsohn JS, Rozema JJ & Iskander DR. Anterior eye surface changes following miniscleral contact lens wear. *Cont Lens Anterior Eye* 2019; 42(1): 70–74.
- Vincent SJ, Alonso-Caneiro D & Collins MJ. Corneal changes following short-term miniscleral contact lens wear. *Cont Lens Anterior Eye* 2014; 37(6): 461–468.
- Vincent SJ, Alonso-Caneiro D & Collins MJ. Miniscleral lens wear influences corneal curvature and optics. *Ophthalmic Physiol Opt* 2016; 36(2): 100–111.
- Serramito M, Carpena-Torres C, Carballo J, Piñero D, Lipson M & Carracedo G. Anterior corneal curvature and aberration changes after scleral lens wear in keratoconus patients with and without ring segments. *Eye Contact Lens* 2018; 45(2): 141–148.
- Soeters N, Visser ES, Imhof SM & Tahzib NG. Scleral lens influence on corneal curvature and pachymetry in keratoconus patients. *Cont Lens Anterior Eye* 2015; 38(4): 294–297.
- Jesus DA & Iskander DR. Assessment of corneal properties based on statistical modeling of OCT speckle. *Biomed Opt Express* 2017; 8(1): 162–176.
- Jesus DA, Majewska M, Krzyzanowska-Berkowska P & Iskander DR. Influence of eye biometrics and corneal micro-structure on noncontact tonometry. *PLoS One* 2017; 12: e0177180.
- Shetty R, Francis M, Shroff R *et al.* Corneal biomechanical changes and tissue remodeling after SMILE and LASIK. *Invest Ophthalmol Vis Sci* 2017; 58: 5703–5712.
- Iskander DR, Kostyszak MA, Jesus DA, Majewska M, Danilewska ME & Krzyzanowska-Berkowska P. Assessing corneal speckle in optical coherence tomography. *Optom Vis Sci* 2020; 97(2): 62–67.
- Consejo A, Gławdecka K, Karnowski K *et al.* Corneal properties of keratoconus based on scheimpflug light intensity distribution. *Invest Ophthalmol Vis Sci* 2019; 60(8): 3197–203.
- Consejo A, Solarski J, Karnowski K, Rozema JJ, Wojtkowski M & Iskander DR. Keratoconus detection based on a single Scheimpflug image. *Transl Vis Sci Technol* 2020;9(7):36.
- Mountford J. *KATT Fitting Instructions*. 2011. [https://www.capcl.com.au/wp-content/uploads/rgp\\_designs/Katt.pdf](https://www.capcl.com.au/wp-content/uploads/rgp_designs/Katt.pdf) (Accessed 27/06/2020)
- Ritzmann M, Caroline PJ, Börret R & Korszen E. An analysis of anterior scleral shape and its role in the design and fitting of scleral contact lenses. *Cont Lens Anterior Eye* 2018; 41: 205–213.
- Li HF, Petroll WM, Møller-Pedersen T *et al.* Epithelial and corneal thickness measurements by in vivo confocal

- microscopy through focusing (CMTF). *Curr Eye Res* 1997; 16: 214–221.
28. Lee A, Karamichos D, Onochie OE *et al.* Hypoxia modulates the development of a corneal stromal matrix model. *Exp Eye Res* 2018; 170: 127–137.
  29. Meek KM & Knupp C. Corneal structure and transparency. *Prog Retin Eye Res* 2015; 49: 1–16.
  30. Clark JI. Order and disorder in the transparent media of the eye. *Exp Eye Res* 2004; 78: 427–432.
  31. Meek KM, Leonard DW, Connon CJ, Dennis S & Khan S. Transparency, swelling and scarring in the corneal stroma. *Eye* 2003; 17(8): 927–936.
  32. Aghamohammadzadeh H, Newton RH & Meek KM. X-ray scattering used to map the preferred collagen orientation in the human cornea and limbus. *Structure* 2004; 12(2): 249–256.
  33. Douth J, Quantock AJ, Smith VA & Meek KM. Light transmission in the human cornea as a function of position across the ocular surface: theoretical and experimental aspects. *Biophys J* 2008; 95(11): 5092–5099.
  34. Boote C, Kamma-Lorger CS, Hayes S *et al.* Quantification of collagen organization in the peripheral human cornea at micron-scale resolution. *Biophys J* 2011; 101(1): 33–42.
  35. Weibull W. A statistical distribution function of wide applicability. *J Appl Mech* 1951; 18(3): 293–297.
  36. Danuser G & Stricker M. Parametric model fitting: From inlier characterization to outlier detection. *IEEE Trans Pattern Anal Mach Intell* 1998; 20(3): 263–280.
  37. Hess RF & Garner LF. The effect of corneal edema on visual function. *Invest Ophthalmol Vis Sci* 1977; 16(1): 5–13.
  38. Mitchell S & Elliott DB. Light scatter changes due to corneal oedema and contact lens wear. *J British Cont Lens Assoc* 1991; 14(4): 183–187.
  39. van den Berg TJ. Intraocular light scatter, reflections, fluorescence and absorption: what we see in the slit lamp. *Ophthalmic Physiol Opt* 2018; 38(1): 6–25.
  40. Wang J, Simpson TL & Fonn D. Objective measurements of corneal light-backscatter during corneal swelling, by optical coherence tomography. *Invest Ophthalmol Vis Sci* 2004; 45(10): 3493–3498.